frontiers | Frontiers in Marine Science

ORIGINAL RESEARCH
published: 02 June 2022
doi: 10.3389/fmars.2022.907527

Potential Phosphorus Uptake Mechanisms in the Deep Sedimentary Biosphere

Delphine Defforey[1], Benjamin J. Tully[2], Jason B. Sylvan[3], Barbara J. Cade-Menun[4], Brandi Kiel Reese[5,6], Laura Zinke[2] and Adina Paytan[1,7]**

[1] Department of Earth and Planetary Sciences, University of California, Santa Cruz, Santa Cruz, CA, United States, [2] Department of Biological Sciences, University of Southern California, Los Angeles, CA, United States, [3] Department of Oceanography, Texas A&M University, College Station, TX, United States, [4] Agriculture and Agri-Food Canada, Swift Current Research and Development Centre, Swift Current, SK, Canada, [5] School of Marine and Environmental Sciences, University of South Alabama, Mobile, AL, United States, [6] Dauphin Island Sea Lab, Dauphin Island, AL, United States, [7] Institute of Marine Sciences, University of California, Santa Cruz, Santa Cruz, CA, United States

OPEN ACCESS

Edited by:
Travis Blake Meador,
Academy of Sciences of the Czech Republic (ASCR), Czechia

Reviewed by:
Beverly E. Flood,
University of Minnesota Twin Cities, United States
Matthew John Harke,
Gloucester Marine Genomics Institute (GMGI), United States

***Correspondence:**
Delphine Defforey
defforey@gmail.com
Adina Paytan
apaytan@ucsc.edu

Specialty section:
This article was submitted to Marine Biogeochemistry, a section of the journal Frontiers in Marine Science

Received: 29 March 2022
Accepted: 26 April 2022
Published: 02 June 2022

Citation:
Defforey D, Tully BJ, Sylvan JB, Cade-Menun BJ, Kiel Reese B, Zinke L and Paytan A (2022) Potential Phosphorus Uptake Mechanisms in the Deep Sedimentary Biosphere. Front. Mar. Sci. 9:907527. doi: 10.3389/fmars.2022.907527

Our understanding of phosphorus (P) dynamics in the deep subseafloor environment remains limited. Here we investigate potential microbial P uptake mechanisms in oligotrophic marine sediments beneath the North Atlantic Gyre and their effects on the relative distribution of organic P compounds as a function of burial depth and changing redox conditions. We use metagenomic analyses to determine the presence of microbial functional genes pertaining to P uptake and metabolism, and solution ^{31}P nuclear magnetic resonance spectroscopy (^{31}P NMR) to characterize and quantify P substrates. Phosphorus compounds or compound classes identified with ^{31}P NMR include inorganic P compounds (orthophosphate, pyrophosphate, polyphosphate), phosphonates, orthophosphate monoesters (including inositol hexakisphosphate stereoisomers) and orthophosphate diesters (including DNA and phospholipid degradation products). Some of the genes identified include genes related to phosphate transport, phosphonate and polyphosphate metabolism, as well as phosphite uptake. Our findings suggest that the deep sedimentary biosphere may have adapted to take advantage of a wide array of P substrates and could play a role in the gradual breakdown of inositol and sugar phosphates, as well as reduced P compounds and polyphosphates.

Keywords: Marine Sediments, P-NMR, deep biosphere, P substrate, metagenome

1 INTRODUCTION

Phosphorus (P) is a key macronutrient for life involved in the structure of nucleic acids in the form of a phosphate–ester backbone, and in the transmission of chemical energy in the form of adenosine triphosphate (ATP). Phosphorus is also a structural constituent in many cell components such as phosphoproteins, and phospholipids in cell membranes. In addition, P is involved in many cellular processes through the mechanism of phosphorylation, which alters the function and activity of

proteins. Hence, P plays an important role in sustaining microbial life in the deep subseafloor environment. This environment is estimated to comprise as many prokaryotic cells as the marine water column and soils, and includes significant prokaryotic populations at depths greater than two kilometers (Roussel et al., 2008; Kallmeyer et al., 2012; Inagaki et al., 2015). Estimates based on cell counts from both ocean margins and oligotrophic ocean gyres sediments suggest that the deep sedimentary subseafloor biosphere could contain 0.18-3.6% of Earth's total biomass and an equal amount of microbial cells as the marine water column (Kallmeyer et al., 2012). The existence and activity of deep subseafloor sediment microbial populations are likely to have profound implications on global biogeochemical cycles and our understanding of the limits of life. However, there is a substantial knowledge gap regarding the nature of P compounds sustaining life in oligotrophic open ocean sediments, and how microbial activity impacts the relative distribution of P compounds in general, especially organic P compounds, in marine sediments. Furthermore, little is known about the impact of the deep biosphere on sedimentary P cycling and P diagenetic processes. This is largely because of analytical difficulties associated with studying P cycling, particularly organic P, in deep ocean sediments that contain low concentrations of organic matter (Ruttenberg, 2014). Therefore, a better understanding of the mechanisms used by deep subseafloor microbes to obtain this essential nutrient is needed.

This study's field site is located at North Pond, an approximately 8 × 15 km sediment-filled basin located on the western flank of the Mid-Atlantic ridge sampled during IODP Expedition 336 (Expedition 336 Scientists, 2012a). Such sediment ponds surrounded by high relief topography are common to the western flank of the Mid-Atlantic Ridge, and are thought to be representative of slow-spreading ridge flank environments (Becker et al., 2001). Sediments at North Pond are predominantly nannofossil ooze with layers of coarse foraminiferal sand and occasional pebble-sized clasts of basalt, serpentinite, gabbroic rocks, and bivalve debris (Expedition 336 Scientists, 2012a). Organic carbon and nitrogen contents in those sediments are low (Ziebis et al., 2012), and organic P was detected at low concentrations throughout the sediment column using sequential sediment extractions (Defforey and Paytan, 2015). In addition, oxygen penetrates deep in the sediment column, and has a "C" shaped depth profile due to oxygen fluxes from oxygenated seawater at the sediment-seawater interface and oxygenated fluids in the underlying basalt crust, with the middle portion of the cores being suboxic to anoxic (Orcutt et al., 2013). Deep sea, carbon-depleted sediments such as the ones sampled in this study represent approximately 70% of the seafloor (Mewes et al., 2016).

In this study, we present metagenomic data from a sediment sample collected at 59 m below seafloor (mbsf), as well as solution ^{31}P nuclear magnetic resonance spectroscopy (^{31}P NMR) data from two depths in the sediment column (3.2 and 56.7 mbsf). The combination of these data yields insights into putative P uptake mechanisms and transformations of P substrates by deep subseafloor microorganisms. This work also improves our knowledge of the role deep subseafloor bacteria play in P cycling and our understanding of the chemical composition of organic P in organic-lean oligotrophic sediments.

2 MATERIALS AND METHODS

2.1 Sample Collection and Storage

The sediment samples used in this study were collected from Site U1382 (Hole U1382B) at North Pond using the advanced piston corer during IODP Expedition 336 in October-November 2011 (**Figure 1**). Site U1382 is located in the southeastern part of North Pond, where sediments are approximately 90 m thick (Expedition 336 Scientists, 2012b). The samples used for this study were U1382B 1H-3, from the oxic portion of the sediment column [average depth 3.2 mbsf, 30 μM dissolved oxygen (DO)] and U1382B 7H-5 (average depths 56.7 mbsf, 1 μM DO; Orcutt et al., 2013). Samples from both depths were used for ^{31}P NMR spectroscopy, while sample U1382B 7H-5 from the suboxic part of the sediment column was used for metagenomic analyses due to problems with the shallow sample during sequencing. Fluorescent microspheres (Fluoresbrite Carboxylate Microspheres; Polysciences, Inc., 15700) were used in every recovered core to monitor any potential contamination (Expedition 336 Scientists, 2012a). Upon recovery, whole-round sediment cores including the sample used here for metagenomic analyses were sectioned on the catwalk, capped

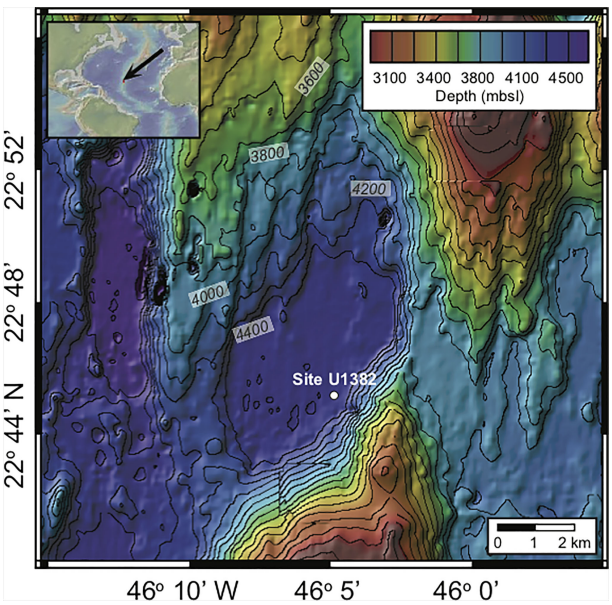

FIGURE 1 | Location of the North Pond field site, located beneath the North Atlantic Gyre. The color scales indicate water depth for each site in meters below sea level (mbsl). Contour line intervals are 100 m for North Pond and the location of Site U1382 is indicated with a white dote. Map created using the default Global Multi-Resolution Topography Synthesis basemap (Ryan et al., 2009) in *GeoMapApp* version 3.6.0 (http://www.geomapapp.org).

and stored at −80°C in sterile bags (Expedition 336 Scientists, 2012c). The sediment samples used for ^{31}P NMR analyses were squeezed-cakes stored at −80°C after porewater collection immediately following core retrieval.

2.2 DNA Extraction and Sequencing

2.2.1 DNA Extraction

The method described in Mills et al. (2012) as modified by B. Kiel Reese for nucleic acids in low biomass open ocean sediments (Kiel Reese et al., 2018) was used to extract DNA. The interior of the whole-round core for sample U1382B 7H-5 was subsampled using sterile techniques and was divided into 25 splits, each weighing ~0.5 g. Initial cell lysis was achieved using five cycles of freeze (liquid nitrogen), thaw (55°C water bath) and vortex steps while stabilizing nucleic acids in a Tris–EDTA–glucose buffer. This step was followed by the addition of lysozyme to the buffer and incubation at 30°C for 10 minutes. Samples were then treated twice with buffered phenol, chloroform and isoamyl alcohol (25:24:1; pH 8.0), and sodium dodecyl sulfate to dissolve the cell membrane and solubilize both high and low molecular weight proteins. Nucleic acids within the aqueous layer above the phenol–chloroform layer were then precipitated in an ethanol and sodium acetate solution. The ethanol solution was decanted following centrifugation of samples at 4°C. Lastly, DNA pellets were resuspended in sterile water, combined into one sample. We quantified the DNA content using a Quibit fluorometer (Thermo Scientific, Waltham, MA, USA) and assessed its quality on a NanoDrop 1000 Spectrophotometer (Thermo Scientific, Waltham, MA, USA) prior to sequencing at the Marine Biological Laboratory Keck facility (Woods Hole, MA, USA). Extraction blanks were included with each sample extraction and yielded no measurable DNA on NanoDrop or Qubit, or observable DNA following PCR and gel electrophoresis.

2.2.2 Sequencing

Metagenome library construction and sequencing was performed through the Deep Carbon Observatory's Census of Deep Life program on an Illumina HiSeq platform. The metagenome sequences can be accessed through the Marine Biological Lab's Visualization and Analysis of Microbial Population Structures database (Huse et al., 2014).

2.3 Bioinformatic Analyses

Raw reads were quality controlled using cutadapt (-e 0.08 –overlap=3; v1.7.1) and Trimmomatic (SLIDINGWINDOW:10:28 MINLEN:75; v0.33). The QCed sequences were searched for SSU rRNA fragments using Meta-RNA (v.H3). SSU rRNA fragments were assembled using EMIRGE (v.1.3) utilizing SILVA SSU as the reference database using the SINA web portal aligner (Ludwig et al., 2004; Capella-Gutiérrez et al., 2009; Pruesse et al., 2012). For sample U1382B 7H-5, 23 full-length SSU rRNAs were reconstructed. Taxonomy was assigned to these assemblies using the mothur (v.1.3.7) commands align.seqs and classify.seqs and SILVA SSU as the reference database. The quality-checked (QCed) sequence library was aligned to its assembled SSU rRNAs using Bowtie2 (v2.2.5). Based on the total number of QCed sequences that aligned to the SSU rRNAs, a length-normalized relative abundance value was determined. Results showed that the sample contained some degree of human-related contamination, both from human DNA (~2%) and human microbiome DNA (~6.7%). In order to verify that the functional genes related to P metabolism were not from human microbiome DNA sequences, we constructed a 16S rRNA gene phylogenetic tree from the metagenome to help determine the origin of microbial taxa (see methods below; **Supplementary Figure 1**). Those most closely related to environmental taxa were considered valid, while those similar to known contaminants, such as common components of the human skin microbiome, were considered contaminants. We also excluded any sequences from the known human microbiome (*Propionobacterium*, *Microbacteriaceae*), as well as sequences without high-level taxonomic assignment from the Proteobacteria (that could include *Enterobacteriaceae*). The QCed sequence library was assembled using IDBA-UD (v.1.1.1), but the overall quality of these assemblies was low (contigs: 49614 n 50: 467 max: 48419 mean: 461). A second round of assembly using all of the contigs from the IDBA-UD output was performed using the Geneious *De Novo* assembler (v.6.3.8; Kearse et al., 2012). This step generated a total of approximately 130 contigs >2.5kb in length. This number was too small for genome binning analysis. To identify genes within the assembled dataset related to P metabolism, all putative coding DNA sequences (CDSs) were determined using Prodigal (v2.6.3), using the metagenome option (-p meta). The identified CDS were compared to the FOAM KEGG database (Prestat et al., 2014) using hmmsearch (Eddy, 2011; v3.1b2; parameters, –cut_tc –notextw) and P-related KO matches were extracted from the output. Additionally, a collection of proteins related to P metabolism collected from UniProtKB were compared to the predicted CDSs using BLASTP (Camacho et al., 2009; v 2.2.30+, parameters, e-value of 1×10^{-20}, max_target_seqs 1).

2.4 16S rRNA Phylogenetic Tree

Full-length 16S rRNA gene sequences were generated using EMIRGE (as described above) and were greater than 1,000 bp in length, with the exception of ID 973 due to poor resolution within the sequence. The sequences were aligned to the SILVA SSU reference database using the SINA web portal aligner (https://www.arb-silva.de/aligner/; Ludwig et al., 2004; Capella-Gutiérrez et al., 2009; Pruesse et al., 2012). These alignments were loaded in to ARB (v6.0.3), manually assessed and added to the non-redundant 16S rRNA gene database (SSURef123 NR99) using ARB Parsimony (Quick) tool (parameters: default). We identified a selection of the nearest neighbors to the sediment metagenome sequences to be used to construct a 16S rRNA gene phylogenetic tree. We also identified additional sequences related to the environmental 16S rRNA gene using a BLAST search against the NCBI RefSeq and non-redundant databases. Environment and reference 16S rRNA gene sequences were aligned using MUSCLE (v3.8.31; parameters: -maxiters 8), processed by the automated trimming program trimAL (v1.2rev59; parameters: -automated1), and aligned for a second time using MUSCLE (parameters: -maxiters 8). The alignment was used to construct an approximate maximum-likelihood phylogenetic tree using FastTree (v2.1.3; parameters: -nt -gtr –gamma; Price et al., 2010).

2.5 Solution ^{31}P NMR Extraction

2.5.1 Sample Extraction

Two sediment samples, U1382B 1H-3 (3.2 mbsf) and 7H-5 (56.7 mbsf), were processed following the method described in Defforey et al. (2017). This method quantitatively removes orthophosphate prior to the alkaline extraction for solution ^{31}P NMR to amplify the signal of low-abundance P compounds, including organic P, relative to that of orthophosphate so that these P forms in oligotrophic sediments may be resolved without the need for extremely long (>24 h) NMR experiments. Briefly, each freeze-dried, ground and sieved sample (<125 μm) was divided into eight splits (1.5 g each). Sample splits were extracted in a citrate–dithionite–bicarbonate buffer to solubilize P bound to iron (Fe) oxyhydroxides (8 h; pH 7.6), after which the sediment residues were washed with ultrapure water (18.2 MΩ·cm deionized water; 2 h). The sediment residues were then extracted in a sodium acetate buffer (6 h; pH 4.0) to solubilize P bound to carbonate fluorapatite, and washed with ultrapure twice (2 h each). After this step, the 8 splits for each sample were combined and extracted in 0.25 M NaOH + 0.05 M Na_2EDTA for 6 h and then centrifuged. Sediment residues were ashed at 550°C and extracted in 0.5 M sulfuric acid (16 h) to determine residual P content, and the NaOH-EDTA extracts were frozen and lyophilized. Prior to solution ^{31}P NMR analysis, lyophilized extracts were redissolved in 500 μL D_2O, H_2O, NaOH–EDTA and 10 M NaOH.

2.5.2 Solution ^{31}P NMR Analysis and Post-Experimental Processing

Spectra were acquired immediately following sample preparation on a Varian Unity INOVA 600 MHz spectrometer equipped with a 10 mm broadband probe [operated by the Stanford Magnetic Resonance Laboratory at Stanford University]. The analytical parameters used were: 20°C, 90° pulse, 0.48 s acquisition time, 4.52 s delay time, 5600 scans (8 h experiments), no spin and an external H_3PO_4 standard. No proton decoupling was used out of concern for sample degradation (Cade-Menun and Liu, 2014). We used the ratio of P concentration to Fe plus manganese (Mn) concentrations (P/Fe+Mn) as a proxy to estimate spin-lattice relaxation times (T_1) to ensure adequate delays between pulses and thus quantitative spectra (McDowell et al., 2006; Cade-Menun and Liu, 2014). We used 5 s recycle delays, which correspond to three to five times the calculated T_1 values. Peak identification was based on spiking with known compounds (α- and β-glycerophosphate) and on literature values (Cade-Menun, 2015). Monoester 1 refers to unidentified orthophosphate monoesters located between 7.5–6.1 ppm, while monoesters 2 and 3 include peaks between 5.7–3.5 ppm and 3.5–2.5 ppm respectively (Cade-Menun, 2017). We processed ^{31}P NMR data using the NMR Utility Transform software (NUTS, Acorn NMR) and calculated peak areas by integration of spectra processed with a 7 Hz line broadening for the full spectrum and 2 Hz line broadening for the monoester region following baseline correction, peak picking and phasing.

2.5.3 Supernatant P Analyses

We measured total P concentrations in sediment extracts using inductively coupled plasma optical emission spectroscopy (ICP-OES) [Perkin-Elmer Optima 4300 DV Inductively Coupled Plasma Optical Emission Spectrometer operated by the University of California, Santa Cruz]. Standards were prepared with the same solutions as those used for the extraction procedure and ranged from 0 – 320 μM P. The detection limit for P on this instrument for both wavelengths is 0.4 μM. We measured molybdate reactive P concentrations (MRP, which includes primarily free orthophosphate) on a QuikChem 8000 automated ion analyzer. Standards were prepared with the same solutions used for the extraction step to minimize matrix effects on P measurements, and ranged from 0 – 30 μM P. The detection limit for P on this instrument is 0.2 μM. We derived molybdate unreactive P concentrations (MUP, which includes primarily organic P and polyphosphates) by subtracting MRP from total P concentrations.

3 RESULTS AND DISCUSSION

3.1 Bioinformatics Data

A target subset of P-related genes was identified in sample U1382B 7H-5 (59.1 mbsf), consisting of 23 genes of interest including phosphate utilization (transport, *pstABS*; metabolism, *phoABDEHR*), phosphonate utilization (transport and metabolism; *phnACDGJ*), phosphite utilization (*ptxABCD*), glycerol 3-phosphate transport (*ugpBC*), polyphosphate metabolism (*ppKX*), and phosphatase activity (*appAB*; **Table 1**; **Supplementary Table 1**). This set of genes was split into two groups. Genes in group 1 (pstABS, ppX, ugpBC, ptxA, phoDR) were present in the FOAM database (accessed April 2016), a curated set of hidden Markov models (HMMs) generated using the KEGG ontology database that could be used to search conserved motifs within the environmental sequences. For FOAM searchable genes of interest (group 1), environmental sequences (excluding *phoR* and *upgC*) were searched using hmmsearch (v3.1b2; parameters, –cut_tc –notextw) with a bit score cutoff of 72 (approximately equivalent to an e-value of 1×10^{-20}). Gene sequences for *phoR* and *upgC* represented protein subunits with generally highly conserved regions: sensor histidine kinases and ATP-binding motifs for ABC-type transporters, respectively. As such, these matches could not be trusted at the same cutoff enforced for the other genes within group 1, and a more stringent cutoff of 105 bit score (approximate e-value equivalent 1×10^{-50}) was used. The results from the FOAM database identified the presence of *ppX* (exopolyphosphatase) and *pstAB*, the ATP-binding and permease subunits of the phosphate ABC-type transporter system. However, the crucial *pstS*, solute-binding subunit, was not identified. Furthermore, even with the more stringent cutoff values, 23 and 38 copies of *upgC* and *phoR* were identified. This large number suggests that even at this cutoff value, a more diverse group of these gene families was identified. The remaining set of genes of interest (group 2), including *ptxABCD*, *ppK*, *phoABED* and *phnACD* were used to search the remaining putative CDS using BLASTP (v 2.2.30+, parameters, e-value of

TABLE 1 | Genes related to P uptake and metabolism identified using metagenomic analyses of sample U1382B 7H-5 (59.1 mbsf).

Gene	Gene name	Taxonomy (MEGAN/RefSeq)
ppX	Exopolyphosphatase	Alphaproteobacteria; Caulobacter, Sphingomonas
ppK	Polyphosphate kinase	Alphaproteobacteria; Bradyrhizobium, Caulobacter, Rhizobiales Actinobacteria; Blastococcus, Curtobacterium
ptxC	Phosphite transport system permease	Alphaproteobacteria; Caulobacter Alphaproteobacteria; Bradyrhizobium Alphaproteobacteria; Methylobacterium
ptxD	NAD-dependent phosphite dehydrogenase	Alphaproteobacteria; Bradyrhizobium, Caulobacter Unclassified
phnA	Phosphonoacetate hydrolase	Alphaproteobacteria; Rhizobiales, Sphingomonas Actinobacteria; Actinomycetales Unclassified
phnD	Phosphonate-binding periplasmic protein	Alphaproteobacteria; Caulobacter
phnJ	C-P lyase	Alphaproteobacteria; Bradyrhizobium, Rhizobiales
phnG	α-D-ribose 1-methylphosphonate 5-triphosphate synthase subunit	Alphaproteobacteria; Bradyrhizobium Alphaproteobacteria; Rhizobiales
appA	Phytase; acid phosphatase	Alphaproteobacteria; Bradyrhizobium, Rhizobiales Actinobacteria; Blastococcus
appB	Alkaline phosphatase	Alphaproteobacteria; Bradyrhizobium Actinobacteria; Curtobacterium
pstA	Phosphate transport system permease	Alphaproteobacteria; Bradyrhizobium, Caulobacter Unclassified
pstB	Phosphate transport system ATP-binding protein	Alphaproteobacteria
phoB	Phosphate regulon response regulator	Alphaproteobacteria; Asticcacaulis, Bradyrhizobium, Caulobacter, Rhizobiales, Rhodopseudomonas, Sphingomonas Betaproteobacteria; Burkholderiales Actinobacteria; Blastococcus, Geodermatophilaceae, Modestobacter Bacterodoites Unclassified
phoD	ABC transporter periplasmic solute-binding protein	Alphaproteobacteria; Bradyrhizobium
phoR	Phosphate regulon sensor histidine kinase	Alphaproteobacteria; Bradyrhizobium, Caulobacter, Phenylobacterium, Sphingomonas Betaproteobacteria; Burkholderia Actinobacteria; Modestobacter Unclassified
ugpC	sn-glycerol 3-phosphate transport system ATP-binding protein	Alphaproteobacteria; Belnapia, Bosea, Bradyrhizobium, Caulobacter, Rhizobiales, Rhizobium Actinobacteria; Geodermatophilaceae, Modestobacter Unclassified

Additional information on the gene IDs can be found in ***Supplementary Table 1****.*

1×10^{-20}, max_target_seqs 1). A total of 187 matches to the environmental sequences were identified. However, the problematic nature of the conserved region within the ATP-binding subunit of the ABC-type transporters resulted in 107 matches to environmental sequences. These were deemed uninformative and were excluded from further analysis. Matches were identified for *appAB*, *phoD*, *phnADGJ*, *ptxCD*, *ppK*. A large portion of the BLAST matches (after ATP-binding subunits) belonged to *phoB* (n = 37), a phosphate regulon response regulator, but this protein family is diverse and multiple types of regulon genes may be identified in this manner. Lastly, for each of the genes identified as related to P uptake and metabolism (both FOAM and BLAST databases), a putative taxonomy was assigned. Putative P-related environmental genes were queried using BLASTP (parameters, e-value 1×10^{-5}, -max_target_seqs 5 -outfmt 5) against the GenBank RefSeq (v75) database. The MEGAN (v4) Last Common Ancestor (LCA) algorithm was used to assign a putative taxonomy based on the top five BLAST matches (**Table 1**). Most P related gene sequences belonged to *Alphaproteobacteria*, or to a combination of *Alphaproteobacteria*, *Betaproteobacteria*, *Actinobacteria* and unclassified microorganisms (**Table 1**). The presence of these microorganisms is further confirmed by 16S rRNA sequence data. The metagenomic analyses performed in this study only yield information regarding the presence of functional genes pertaining to P metabolism, and these may represent DNA from active and inactive or dormant microorganisms. Indeed, most phylogenetic groups identified in North Pond sediments have been shown to be inactive (Kiel Reese et al., 2018). However, active *Alphaproteobacteria* (mainly from the *Caulobacteraceae* family and *Brevundimonas* genus) have been found throughout the sediment column at Hole U1382B, as well as some active *Betaproteobacteria* (*Achromobacter* genus) and *Gammaproteobacteria* (*Pseudomonas* genus, and the genera *Stentrophomonas and Methylophaga*; Kiel Reese et al., 2018). This suggests that the functional genes reported in our study are present at depths where microorganisms are active and utilizing P and may thus be impacting sedimentary organic matter remineralization through their metabolic activity.

3.2 P NMR Data

Solution ^{31}P NMR spectra for both samples are shown in **Figure 2** and **Supplemental Figure 2**, and chemical shifts of peaks for compounds and compound classes are shown in

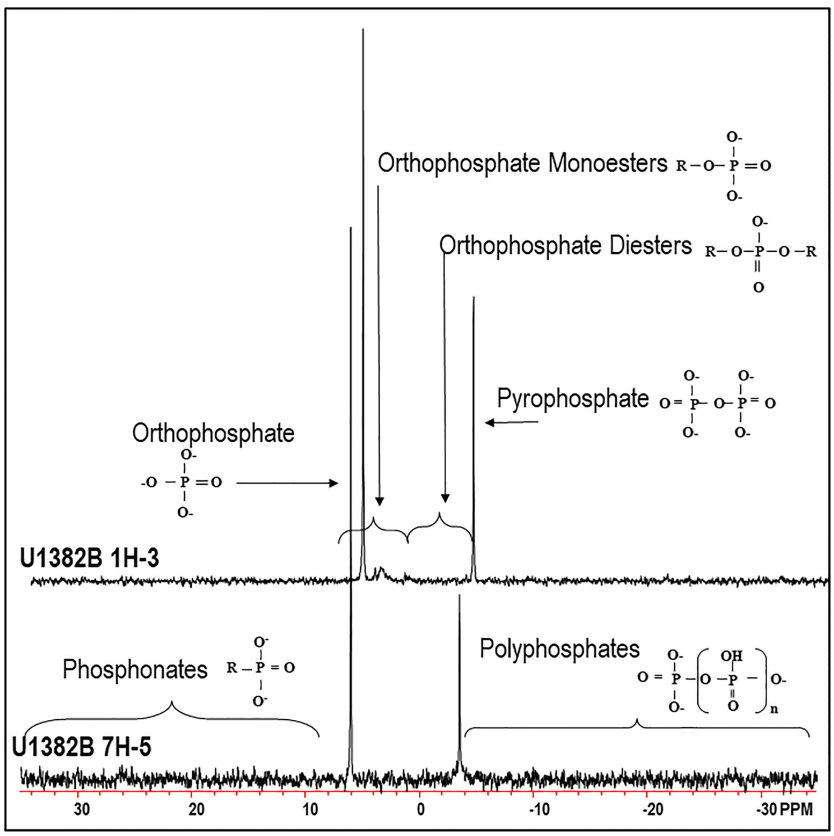

FIGURE 2 | Solution ^{31}P NMR spectrum of sample U1382B 1H-3 (3.2 mbsf, top), and U1382B 7H-5 (56.7 mbsf, bottom). Spectra were processed with 7 Hz line-broadening, and are plotted with the orthophosphate peak at the same height. See **Supplementary Figure 2** for more details of the orthophosphate monoester region.

Supplementary Table 2. The 2–step pretreatment preceding the alkaline extraction removed 95% of orthophosphate in sample U1382B 1H-3, and 98% in sample U1382B 7H-5 with no measurable MUP removal (**Table 2**; **Figure 3**). For both samples, the 5-s recycle delays were long enough to produce quantitative spectra (**Table 3**). Metal content was similar in both NMR extracts, but P content was lower for the deeper sample (**Table 3**). The shallower, oxic sample (U1382B 1H-3, 3.2 mbsf, 30 µM DO) contained a wider variety of P compounds than the deeper, suboxic sample (U1382B 7H-5, 56.7 mbsf, ~1 µM DO), and a greater concentration of Organic P detected in NMR spectra (**Table 4**). The most abundant P compounds in both samples identified using solution ^{31}P NMR after the 2–step pretreatment were inorganic orthophosphate, pyrophosphate and polyphosphates (**Table 4**; **Figure 2**). Polyphosphates are chains of phosphates linked by anhydrous bonds; pyrophosphates are polyphosphates with only two phosphate groups. Both polyphosphates and pyrophosphates can be associated with living organisms, and can be inorganic or organic; ATP is an example of an organic polyphosphate (Heinonen, 2001; Condron et al., 2005). Pyrophosphate and polyphosphates have been identified by solution ^{31}P NMR in culture-grown algae

TABLE 2 | Extraction yields for each step. P_{red} refers to P solubilized during the reductive step (step 1), P_{CFA} refers to P released during the sodium acetate step (step 2).

Sample ID	Average depth (mbsf)	Porewater MRP (µM)[a]	P_{red} (µmol/g)	P_{CFA} (µmol/g)	NMR extract TP (µmol g^{-1})	Residual P (µmol g^{-1})	Extracted P (%)
U1382B 1H–3	3.2	1.79	9.82	3.88	0.31	0.36	97.5
U1382B 7H–5	56.7	1.35	8.87	3.49	0.13	0.17	98.7

Porewater MRP concentrations are from (Expedition 336 Scientists, 2012d). NMR extract TP corresponds to the total P content in the alkaline extracts (step 3). Extracted P is the fraction of P that was extracted in steps 1-3.

[a]*Expedition 336 scientists [2012].*

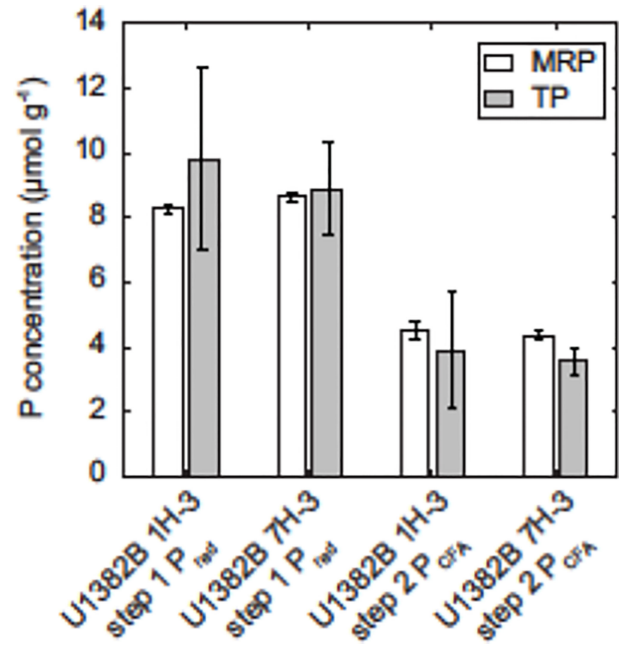

FIGURE 3 | Mean molybdate-reactive P (MRP) and total P content in pretreatment extracts from steps 1 (P_{red}, citrate–dithionite–bicarbonate and water extracts) and 2 (P_{CFA}, sodium acetate and water extracts), along with standard deviations derived from replicate sediment sample splits. Total P concentrations were measured on an ICP-OES, while MRP concentrations were measured colorimetrically on a QuikChem 8000 automated ion analyzer.

(Cade-Menun and Paytan, 2010) in estuary and river sediments (Shan et al., 2016; Watson et al., 2018), and in marine sediments by solid-state and solution ^{31}P NMR (Sannigrahi and Ingall, 2005; Prüter et al., 2020). We also measured small amounts of organic P compounds, including phosphonates (reduced organic P compounds with a direct C–P bond), and orthophosphate monoesters and diesters (**Table 4**; **Figure 2**). Orthophosphate monoesters were the most abundant forms of organic P in both samples, which is consistent with numerous studies that have shown them to generally be the dominant group of organic P compounds in both marine and terrestrial environments (Ingall et al., 1990; Carman et al., 2000; Paytan et al., 2003; Sannigrahi and Ingall, 2005; Turner et al., 2005; Shan et al., 2016; Watson et al., 2018; Prüter et al., 2020). In the shallower sample, we were able to resolve individual peaks in the orthophosphate monoester region and identify a number of different monoester compounds (**Table 4**). Among them, the most abundant monoester compounds identified were the inositol hexakisphosphate (IHP) stereoisomers *myo*- and *scyllo*-IHP. Inositol phosphates form the dominant class of organic P compounds in soils, and are abundant in aquatic systems (Turner et al., 2002). Of all IHP stereoisomers, *myo*-IHP is the most abundant, but *scyllo*-, *D-chiro*- and *neo*-IHP have also been measured in soils and marine sediments (White and Miller, 1976; Turner et al., 2012). Peaks consistent with *D-chiro*- and *neo*-IHP were detected in the Monoester 1 region of these spectra (**Supplementary Table 1**), but were not specifically identified due to uncertainties about peak identification and low concentrations. Peaks for α- and β–glycerophosphate were also identified in the spectrum of the shallower sample. Although these are included with orthophosphate monoesters, they are artifacts from degradation during extraction and analysis, from phospholipids in the original samples, which are orthophosphate diesters (Cade-Menun, 2015). As such, they were included in the calculation for total orthophosphate diesters rather than total orthophosphate monoesters (**Table 4**). Peaks for DNA were identified in the orthophosphate diester region of spectra for both depths (**Table 4**). Other peaks in the orthophosphate diester region are consistent with phospholipids (**Supplementary Table 2**; Cade-Menun, 2015), but were not specifically identified.

3.3 Combining Metagenomic and P NMR Data

The combined use of metagenomic analyses and solution ^{31}P NMR spectroscopy yields valuable information regarding P cycling by deep sedimentary subseafloor microorganisms, as well as microbial P uptake mechanisms. While we do not have a metagenome for the shallower sediments at Hole U1382B, the decrease in abundance of organic and biogenic P compounds (**Table 4**) suggests that deep sedimentary subseafloor microorganisms are utilizing those compounds as a P source, and possibly as an organic C source in this C-depleted environment (Heath, 2005; Ziebis et al., 2012). Decreases in organic P may also scale with a decrease in cell density; further research is warranted.

In the shallow sample, *myo*-IHP can adsorb on the same sites of Fe and aluminum (Al) oxides as phosphate anions since adsorption occurs through the phosphate groups *via* ligand exchange with surrounding porewater and hydroxide groups on mineral surfaces (Goldberg and Sposito, 1985; Baldwin et al., 2002; Celi and Barberis, 2005; Gérard, 2016). Little is known regarding possible differences in the behavior of other stereoisomeric forms of IHP, but they may adsorb on oxide surfaces in a similar manner as *myo*-IHP. Once sorbed on short-range ordered Al precipitates, *myo*-IHP and other P compounds, including sugar phosphates such as glucose 6-phosphate have been shown to be poorly available to microorganisms (Shang et al., 1996), which would allow them to

TABLE 3 | Aluminum, calcium, iron, potassium, magnesium, manganese and phosphorus content in ^{31}P NMR extracts.

Sample ID	Depth (mbsf)	Al	Ca	Fe	K	Mg	Mn	P	P/(Fe+Mn)	Calculated T_1 (s)
		µmol g^{-1}								
U1382B 1H–3	3.2	1.16	8.86	0.03	0.03	1.05	0.02	0.31	3.01	1.17
U1382B 7H–5	56.7	0.68	8.86	0.02	0.02	0.33	0.01	0.13	2.00	0.89

T_1 values are derived from P to iron and manganese ratios (w/v) using the relationship derived by McDowell et al. (2006).

TABLE 4 | Phosphorus compounds or compound classes identified from ^{31}P NMR spectral analyses of samples U1382B 1H-3 (3.2 mbsf) and 7H-5 (56.7 mbsf).

P Compounds or Compound Classes	U1382B 1H-3 (nmol g^{-1})	% of sample TP	U1382B 7H-5 (nmol g^{-1})	% of sample TP
Total NMR Inorganic P	238.4	1.62	110.4	0.86
Orthophosphate	149	1.01	60.3	0.47
Pyrophosphate	75.6	0.51	37.4	0.29
Polyphosphates	14.0	0.09	12.6	0.10
Total NMR Organic P	71.6	0.49	19.6	0.15
Phosphonates	6.51	0.04	6.76	0.05
Total Orthophosphate Monoesters	51.8[a]	0.35[a]	10.9[a]	0.09[a]
α-glycerophosphate	1.55	0.01	–	–
β-glycerophosphate	3.10	0.02	–	–
scyllo-IHP[b]	3.10	0.02	–	–
myo-IHP (phytate)[b]	9.30	0.06	–	–
Monoester1	9.30	0.06	2.73	0.02
Monoester 2	27.0	0.18	6.37	0.05
Monoester 3	3.10	0.02	1.82	0.01
Total Orthophosphate Diesters	17.1[a]	0.12[a]	8.32[a]	0.06[a]
DNA	2.89	0.02	0.39	<0.01
Other diesters	5.89	0.04	1.56	0.01
Ester : Phosphonate ratio[c]	10.0		1.90	

The percentage values reported are relative to total sample P, including P removed during the 2–step pretreatment, and residual P.
[a]*Corrected for diester degradation products (α- and β-glycerophosphate) that appear in the monoester region in P-NMR spectra.*
[b]*IHP, inositol hexaphosphate.*
[c]*Ratio of (total orthophosphate monoesters + total orthophosphate diesters) to phosphonates.*

persist at depth in marine sediments. However, surface properties of oxides are modified when associated with other minerals such as clay minerals, which affect their interactions with organic P and may weaken the complex formed with oxides (Celi et al., 2003), thus increasing their bioavailability. In addition to sorption on Fe and Al oxides, *myo*-IHP can form soluble complexes with calcium in calcareous sediments, which may enhance the interactions between *myo*-IHP and calcium-bearing minerals and further stabilize it (Celi and Barberis, 2005). The bioavailability of organic P compounds is primarily dependent on the stability of the phosphate surface complexes rather than by the total amount of phosphate adsorbed (Shang et al., 1996). Varying redox conditions have been shown to strongly regulate IHP remineralization, and lead to enhanced IHP decomposition under anaerobic conditions (Suzumura and Kamatani, 1995), and the presence of the appA gene, associated with phytase (Liu et al., 2018) is consistent with mineralization of IHP compounds. The observed decrease in orthophosphate monoester abundance with depth was also reported by Prüter et al. (2020) for sediments of the Baltic Sea, who also reported a decrease in orthophosphate monoesters with distance from the coast. These decreases could be due to decreases in cell density, or to an increase in bioavailability of those compounds resulting from the transition to suboxic conditions in the middle parts of the sediment column (Zhang et al., 1994; **Table 4**, **Figure 2**). Indeed, bacteria at this depth possess genes encoding for phosphomonoesterases, (*appA, appB, phoD*; Vershinina and Znamenskaya, 2002) and could utilize those deeply buried P compounds as they become more susceptible to enzymatic hydrolysis.

Orthophosphate diesters were also present at both depths as DNA in both samples, phospholipid degradation products in the shallow sample, and other diesters in both samples (**Table 4**, **Figure 2**). These compounds may originate from living organisms, and DNA may also be retained by sorption. The sorption of nucleic acids on mineral surfaces is affected by the molecular weight of DNA, the presence of montmorillonite, pH and redox conditions (Greaves and Wilson, 1969; Celi and Barberis, 2005; Condron et al., 2005). The complexed nucleic acid forms with montmorillonite are weaker than those with *myo*-IHP due to the presence of a single hydroxide group available for ligand exchange (Greaves and Wilson, 1969). This makes nucleic acids more vulnerable to microbial enzymatic hydrolysis (Greaves and Wilson, 1970). The decrease in orthophosphate diester abundance with depth and the presence of genes such as *phoD* and *ugpC* suggest putative mechanisms for the uptake of orthophosphate diesters (*phoD*) and glycerophosphoryl diesters (*ugpC*) at Site U1382 (Wanner, 1993; Vershinina and Znamenskaya, 2002).

Other potential sources of P, and possibly C, to the deep biosphere are phosphonates, which we measured both in shallow and deeper sediments (**Table 4**, **Figure 2**). While previously thought to be refractory, these compounds have been shown to be as bioavailable as phosphate esters, especially under anoxic conditions (Benitez-Nelson et al., 2004) and represent a potential source of both P and organic C to the deep biosphere (Sosa et al., 2019). Indeed, a number of genes pertaining to phosphonate utilization were identified in our sample: *phnA* (phosphonoacetate hydrolase), *phnD* (phosphonate-binding periplasmic protein), *phnJ* (component of C-P lyase complex) and *phnG* (component of C-P lyase complex; **Table 1**). The comparable phosphonate abundance (6.51 and 6.76 nmol g^{-1} at both depths), the high ester to phosphonate ratios that decrease with depth, the presence of genes related to phosphonate utilization and redox conditions shown to enhance phosphonate remineralization (i.e., reducing conditions) suggest that phosphonates represent a likely substrate for deep subseafloor microorganisms at that depth in the sediment column. This is consistent with the results of Sosa et al. (2019) showing that C-P

lyase was more prevalent in ocean regions featuring sustained periods of phosphate depletion.

Small amounts of polyphosphates were measured in both spectra, and genes for exopolyphosphatase (*ppX*) were present in the metagenome (**Table 1**, **Figure 2**). This enzyme catalyzes the hydrolysis of the terminal phosphate group in polyphosphates (Jones et al., 2016, p. 2). We also identified gene sequences for polyphosphate kinase (*ppK*), which catalyzes the reversible synthesis of polyphosphate from nucleoside triphosphates (Jones et al., 2016). Polyphosphates are synthesized by all cells, and play an important role in nutrient storage, regulatory functions and metal chelation (Rao et al., 2009). They also play a key role in nucleating the growth of authigenic carbonate fluorapatite in marine sediments, which has profound implications for reactive P burial (Diaz et al., 2008).

An unexpected result from the metagenomic analyses was the presence of two genes related to phosphite metabolism: *ptxC* and *ptxD*. Phosphite utilization genes have been identified in diverse marine microorganisms, and their abundance is higher in marine environments with low P (Martínez et al., 2012). Furthermore, it was shown that phosphite and phosphonate production in surface waters could contribute to a global P redox cycle (Van Mooy et al., 2015). While we did not measure phosphite in our samples, and, to our knowledge, phosphite has not been measured in open ocean sediments, the presence of reduced organic P in the form of phosphonates and genes related to phosphite utilization raises the possibility of this compound potentially playing a role in P sediment cycling.

4 CONCLUSIONS

In this study, we presented a combination of metagenomics analysis and solution ^{31}P-NMR for studying putative P uptake mechanisms and metabolism, as well as the distribution of organic and biogenic P substrates in deep subseafloor sediments. We demonstrated that diverse organic P compounds persist at depth in sediments underlying oligotrophic marine settings, and that changes in redox conditions may play an important role in increasing their bioavailability. We identified a wide variety of potential P sources to the deep biosphere, as well as putative enzymatic pathways for P uptake and utilization. While this study only provides potential P uptake mechanisms, it sets the stage for future work to investigate the expression of functional genes pertaining to P uptake and metabolism and raises interesting questions about microbial transformations of sedimentary organic and biogenic P.

DATA AVAILABILITY STATEMENT

The datasets presented in this study can be found in online repositories. The names of the repository/repositories and accession number(s) can be found below: https://www.bco-dmo.org/project/664073, 664073.

AUTHOR CONTRIBUTIONS

AP: Conceptualization, Project funding, Data interpretation, Writing. DD: Conceptualization, Analytical work, Data curation, Methodology, Visualization, Writing original draft. BT and JS: Bioinformatics, Metagenomic interpretation, Data curation. BC-M: Methods development, NMR data interpretation, Editing. BKR and LZ: Molecular data analysis and interpretation. All authors have read and approved the final version of this manuscript prior to submission.

FUNDING

Funding was provided by a graduate student fellowship from the Center for Dark Energy Biosphere Investigations (NSF C-DEBI) to DD (award # 157598), a student research grant from the Geological Society of America to DD, a C-DEBI *Research and Travel Exchange Program* grant to DD, a research grant from C-DEBI to AP (award # 15626), sequencing grant to AP, DD, JS and BKR from the Census of Deep Life and internal AAFC funding (J-002238) to BC-M.

ACKNOWLEDGMENTS

We thank the Integrated Ocean Drilling Program and the shipboard scientists and technical staff involved in IODP expedition 336 who collected the sediment samples used in this study. We also thank Dr. Corey Liu, Rob Franks, Michael Kong and Richard Kevorkian for their assistance with this project.

SUPPLEMENTARY MATERIAL

The Supplementary Material for this article can be found online at: https://www.frontiersin.org/articles/10.3389/fmars.2022.907527/full#supplementary-material

REFERENCES

Baldwin, D. S., Mitchell, A. M., and Olley, J. M. (2002). "Pollutant-Sediment Interactions: Sorption, Reactivity and Transport of Phosphorus," in *Agriculture, Hydrology and Water Quality*. Eds. P. M. Haygarth and S. C. Jarvis (Wallingford, UK: CABI Publ), 265–280.

Becker, K., Bartetzko, A., and Davis, E. E. (2001). Leg 174B Synopsis: Revisiting Hole 395A for Logging and Long-Term Monitoring of Off-Axis Hydrothermal Processes in Young Oceanic Crust. In K. Becker and M. J. Malone. (Eds.), *Proc. ODP, Sci.Results*, 174B, 1–13 [Online]. Available at: http://www-odp.tamu.edu/publications/174B_SR/VOLUME/SYNOPSIS/SR174BSY.PDF

Benitez-Nelson, C. R., O'Neill, L., Kolowith, L. C., Pellechia, P., and Thunell, R. (2004). Phosphonates and Particulate Organic Phosphorus Cycling in an Anoxic Marine Basin. *Limnol. Oceanogr.* 49, 1593–1604. doi: 10.4319/lo.2004.49.5.1593

Cade-Menun, B. J. (2015). Improved Peak Identification in ^{31}P-NMR Spectra of Environmental Samples With a Standardized Method and Peak Library. *Geoderma* 257-258, 102–114. doi: 10.1016/j.geoderma.2014.12.016

Cade-Menun, B. J. (2017). Characterizing Phosphorus Forms in Cropland Soils With Solution 31P–NMR: Past Studies and Future Research Needs. *Chem. Biol. Technol. Agric.* 4, 19. doi: 10.1186/s40538-017-0098-4

Cade-Menun, B. J., and Liu, C. W. (2014). Solution phosphorus-31 Nuclear Magnetic Resonance Spectroscopy of Soils From 2005 to 2013: A Review of Sample Preparation and Experimental Parameters. *Soil Sci. Soc Am. J.* 78, 19. doi: 10.2136/sssaj2013.05.0187dgs

Cade-Menun, B. J., and Paytan, A. (2010). Nutrient, Temperature and Light Stress Alter Phosphorus and Carbon Forms in Culture-Grown Algae. *Mar. Chem.* 121, 27–36. doi: 10.1016/j.marchem.2010.03.002

Camacho, C., Coulouris, G., Avagyan, V., Ma, N., Papadopoulos, J., Bealer, K., et al. (2009). BLAST+: Architecture and Applications. *BMC Bioinf.* 10, 421. doi: 10.1186/1471-2105-10-421

Capella-Gutiérrez, S., Silla-Martínez, J. M., and Gabaldón, T. (2009). trimAl: A Tool for Automated Alignment Trimming in Large-Scale Phylogenetic Analyses. *Bioinformatics* 25, 1972–1973. doi: 10.1093/bioinformatics/btp348

Carman, R., Edlund, G., and Damberg, C. (2000). Distribution of Organic and Inorganic Phosphorus Compounds in Marine and Lacustrine Sediments: A 31P NMR Study. *Chem. Geol.* 163, 101–114. doi: 10.1016/S0009-2541(99)00098-4

Celi, L., and Barberis, E. (2005). "Abiotic Stabilization of Organic Phosphorus in the Environment," in *Organic Phosphorus in the Environment*. Eds. B. L. Turner and D. S. Baldwin (Wallingford, UK: CABI Publ), 113–132.

Celi, L., De Luca, G., and Barberis, E. (2003). Effects of Interaction of Organic and Inorganic P With Ferrihydrite and Kaolinite-Iron Oxide Systems on Iron Release. *Soil Sci.* 168, 479–488. doi: 10.1097/01.ss.0000080333.10341.a4

Condron, L. M., Turner, B. L., and Cade-Menun, B. J. (2005). "Chemistry and Dynamics of Soil Organic Phosphorus," in *Phosphorus Agriculture and the Environment*. Eds. J. T. Sims and A. N. Sharpley (Madison, WI, USA: Soil Science Society of America), 87–121.

Defforey, D., Cade-Menun, B. J., and Paytan, A. (2017). A New Solution ^{31}P NMR Sample Preparation Scheme for Marine Sediments. *Limnol. Oceanogr.: Methods* 15, 381–393. doi: 10.1002/lom3.10166\

Defforey, D., and Paytan, A. (2015). Data Report: Characteristics of Sedimentary Phosphorus at North Pond, IODP Expedition 336. *Proc. Integr. Ocean Drill. Program* 336, 1–9. doi: 10.2204/iodp.proc.336.205.2015

Diaz, J., Ingall, E., Benitez-Nelson, C., Paterson, D., de Jonge, M. D., McNulty, I., et al. (2008). Marine Polyphosphate: A Key Player in Geologic Phosphorus Sequestration. *Science* 320, 652–655. doi: 10.1126/science.1151751

Eddy, S. R. (2011). Accelerated Profile HMM Searches. *PloS Comput. Biol.* 7, e1002195. doi: 10.1371/journal.pcbi.1002195

Expedition 336 Scientists (2012a). Initiation of Long-Term Coupled Microbiological, Geochemical, and Hydrological Experimentation Within the Seafloor at North Pond, Western Flank of the Mid-Atlantic Ridge. *IODP Proc.* 336, 1–72. doi: 10.2204/iodp.pr.336.2012

Expedition 336 Scientists (2012b). Site U1382. *Proc. Integr. Ocean Drill. Program* 336, 1–141. doi: 10.2204/iodp.proc.336.104.2012

Expedition 336 Scientists (2012c). Methods. *Proc. Integr. Ocean Drill. Program* 336, 1–87. doi: 10.2204/iodp.proc.336.102.2012

Expedition 336 Scientists (2012d). Sediment and Basement Contact Coring. *Proc. Integr. Ocean Drill. Program* 336, 1–46. doi: 10.2204/iodp.proc.336.106.2012

Gérard, G. (2016). Clay Minerals, Iron/Aluminum Oxides, and Their Contribution to Phosphate Sorption in Soils – A Myth Revisited. *Geoderma* 262, 213–226. doi: 10.1016/j.geoderma.2015.08.036

Goldberg, S., and Sposito, G. (1985). On the Mechanism of Specific Phosphate Adsorption by Hydroxylated Mineral Surfaces: A Review. *Commun. Soil Sci. Plant Anal.* 16, 801–821. doi: 10.1080/00103628509367646

Greaves, M. P., and Wilson, M. J. (1969). The Adsorption of Nucleic Acids by Montmorillonite. *Soil Biol. Biochem.* 1, 317–323. doi: 10.1016/0038-0717(69)90014-5

Greaves, M. P., and Wilson, M. J. (1970). The Degradation of Nucleic Acids and Montmorillonite-Nucleic-Acid Complexes by Soil Microorganisms. *Soil Biol. Biochem.* 2, 257–268. doi: 10.1016/0038-0717(70)90032-5

Heath, R. T. (2005). "Microbial Turnover of Organic Phosphorus in Aquatic Systems," in *Organic Phosphorus in the Environment*. Eds. B. L. Turner, E. Frossard and D. S. Baldwin (Wallingford, UK: CABI Publ), 185–203.

Heinonen, J. (2001). *Biological Role of Inorganic Pyrophosphate* (New York, NY USA: Springer).

Huse, S. M., Welch, D. B. M., Voorhis, A., Shipunova, A., Morrison, H. G., Eren, A. M., et al. (2014). Vamps: A Website for Visualization and Analysis of Microbial Population Structures. *BCM Bioinf.* 14, 41. doi: 10.1186/1471-2105-15-41

Inagaki, F., Hinrichs, K.-U., and Kubo, Y. (2015). Exploring Deep Microbial Life in Coal-Bearing Sediment Down to ~2.5 Km Below the Ocean Floor. *Science* 349, 420–424. doi: 10.1126/science.aaa6882

Ingall, E. D., Schroeder, P. A., and Berner, R. A. (1990). The Nature of Organic Phosphorus in Marine Sediments: New Insights From 31P NMR. *Geochim. Cosmochim. Acta* 54, 2617–2620. doi: 10.1016/0016-7037(90)90248-J

Jones, D. S., Flood, B. E., and Bailey, J. V. (2016). Metatranscriptomic Insights Into Polyphosphate Metabolism in Marine Sediments. *ISME J.* 10, 1015–1019. doi: 10.1038/ismej.2015.169

Kallmeyer, J., Pockalny, R., Adhikari, R. R., Smith, D. C., and D'Hondt, S. (2012). Global Distribution of Microbial Abundance and Biomass in Subseafloor Sediment. *Proc. Natl. Acad. Sci.* 109, 16213–16216. doi: 10.1073/pnas.1203849109

Kearse, M., Moir, R., Wilson, A., Stones-Havas, S., Cheung, M., Sturrock, S., et al. (2012). Geneious Basic: An Integrated and Extendable Desktop Software Platform for the Organization and Analysis of Sequence Data. *Bioinformatics* 28, 1647–1649. doi: 10.1093/bioinformatics/bts199

Kiel Reese, B., Zinke, L. A., Sobol, M. S., LaRoue, D. E., Orcutt, B. N., Zhang, X., et al (2018). Nitrogen Cycling of Active Bacteria Within Oligotrophic Sediment of the Mid-Atlantic Ridge Flank. *Geomicrobiol. J.* 35, 468–483. doi: 10.1080/01490451.2017.1392649

Liu, J., Cade-Menun, B. J., Bainard, L., Yang, J., Hu, Y. F., Liu, C. W., et al. (2018). Long-Term Land Use Affects Phosphorus Speciation and the Composition of Phosphorus Cycling Functional Genes in Agricultural Soils. *Front. Microbiol.* 9. doi: 10.3389/fmicb.2018.01643

Ludwig, W., Strunk, O., Westram, R., Richter, L., Meier, H., Yadhukumar, et al. (2004). ARB: A Software Environment for Sequence Data. *Nucleic Acids Res.* 32, 1363–1371. doi: 10.1093/nar/gkh293

Martínez, A., Osburne, M. S., Sharma, A. K., DeLong, E. F., and Chisholm, S. W. (2012). Phosphite Utilization by the Marine Picocyanobacterium Prochlorococcus Mit9301: Phosphite Utilization by Prochlorococcus Mit9301. *Environ. Microbiol.* 14, 1363–1377. doi: 10.1111/j.1462-2920.2011.02612.x

McDowell, R. W., Stewart, I., and Cade-Menun, B. J. (2006). An Examination of Spin–Lattice Relaxation Times for Analysis of Soil and Manure Extracts by Liquid State phosphorus-31 Nuclear Magnetic Resonance Spectroscopy. *J. Environ. Qual.* 35, 293. doi: 10.2134/jeq2005.0285

Mewes, K., Mogollón, J. M., Picard, A., Rühlemann, C., Eisenhauer, A., Kuhn, T., et al. (2016). Diffusive Transfer of Oxygen From Seamount Basaltic Crust Into Overlying Sediments: An Example From the Clarion–Clipperton Fracture Zone. *Earth Planet. Sci. Lett.* 433, 215–225. doi: 10.1016/j.epsl.2015.10.028

Mills, H. J., Kiel Reese, B., and Peter, C. S. (2012). Characterization of Microbial Population Shifts During Sample Storage. *Front. Microbiol.* 3. doi: 10.3389/fmicb.2012.00049

Orcutt, B. N., Wheat, C. G., Rouxel, O., Hulme, S., Edwards, K. J., and Bach, W. (2013). Oxygen Consumption Rates in Subseafloor Basaltic Crust Derived From a Reaction Transport Model. *Nat. Commun.* 4, 2539. doi: 10.1038/ncomms3539

Paytan, A., Cade-Menun, B. J., McLaughlin, K., and Faul, K. L. (2003). Selective Phosphorus Regeneration of Sinking Marine Particles: Evidence From ^{31}P NMR. *Mar. Chem.* 82, 55–70. doi: 10.1016/S0304-4203(03)00052-5

Prestat, E., David, M. M., Hultman, J., Taş, N., Lamendella, R., Dvornik, J., et al. (2014). Foam (Functional Ontology Assignments for Metagenomes): A Hidden Markov Model (HMM) Database With Environmental Focus. *Nucleic Acids Res.* 42, e145. doi: 10.1093/nar/gku702

Price, M. N., Dehal, P. S., and Arkin, A. P. (2010). FastTree 2 – Approximately Maximum-Likelihood Trees for Large Alignments. *PloS One* 5, e9490. doi: 10.1371/journal.pone.0009490

Pruesse, E., Peplies, J., and Glöckner, F. O. (2012). Sina: Accurate High-Throughput Multiple Sequence Alignment of Ribosomal RNA Genes. *Bioinformatics* 28, 1823–1829. doi: 10.1093/bioinformatics/bts252

Prüter, J., Leipe, T., Michalik, D., Klysubun, W., and Leinweber, P. (2020). Phosphorus Speciation in Sediments From the Baltic Sea, Evaluated by a Multi-Method Approach. *J. Soils Sediments* 20, 1676–1691. doi: 10.1007/s11368-019-02518-w

Rao, N. N., Gómez-García, M. R., and Kornberg, A. (2009). Inorganic Polyphosphate: Essential for Growth and Survival. *Annu. Rev. Biochem.* 78, 605–647. doi: 10.1146/annurev.biochem.77.083007.093039

Roussel, E. G., Bonavita, M.-A. C., Querellou, J., Cragg, B. A., Webster, G., Prieur, D., et al. (2008). Extending the Sub-Sea-Floor Biosphere. *Science* 320, 1046–1046. doi: 10.1126/science.1154545

Ruttenberg, K. C. (2014). "The Global Phosphorus Cycle," in *Treatise on Geochemistry*. 2nd Ed. H. Holland and K. Turekian (Amsterdam: Elsevier), 499–558.

Ryan, W. B. F., Carbotte, S. M., and Coplan, J. O. (2009). Global Multi-Resolution Topography Synthesis. *Geochem. Geophys. Geosystems* 10, Q03014. doi: 10.1029/2008GC002332

Sannigrahi, P., and Ingall, E. (2005). Polyphosphates as a Source of Enhanced P Fluxes in Marine Sediments Overlain by Anoxic Waters: Evidence From P-31 Nmr. *Geochem. Trans.* 6, 52–59. doi: 10.1063/1.1946447

Shang, C., Caldwell, D. E., Stewart, J. W. B., Tiessen, H., and Huang, P. M. (1996). Bioavailability of Organic and Inorganic Phosphates Adsorbed on Short-Range Ordered Aluminum Precipitate. *Microb. Ecol.* 31, 29–39. doi: 10.1007/BF00175073

Shan, B., Li, J., Zhang, W. Q., Di, Z., and Jin, X. (2016). Characteristics of Phosphorus Components in the Sediments of Main Rivers Into the Bohai Sea. *Ecol. Engineer.* 97, 426–433. doi: 10.1016/j.ecoleng.2016.10.042

Sosa, O. A., Repeta, D. J., DeLong, E. F., Ashkezari, M. D., and Karl, D. M. (2019). Phosphate-Limited Ocean Regions Select for Bacteria Populations Enriched in the Carbon-Phosphorus Lyase Pathway for Phosphonate Degradation. *Environ. Microbiol.* 21, 2402–2412. doi: 10.1111/1462-2920.14628

Suzumura, M., and Kamatani, A. (1995). Mineralization of Inositol Hexaphosphate in Aerobic and Anaerobic Marine Sediments: Implications for the Phosphorus Cycle. *Geochim. Cosmochim. Acta* 59, 1021–1026. doi: 10.1016/0016-7037(95)00006-2

Turner, B. L., Cade-Menun, B. J., Condron, L. M., and Newman, S. (2005). Extraction of Soil Organic Phosphorus. *Talanta* 66, 294–306. doi: 10.1016/j.talanta.2004.11.012

Turner, B. L., Cheesman, A. W., Godage, H. Y., Riley, A. M., and Potter, B. V. L. (2012). Determination of Neo- and D-Chiro-Inositol Hexakisphosphate in Soils by Solution ^{31}P NMR Spectroscopy. *Environ. Sci. Technol.* 46, 4994–5002. doi: 10.1021/es204446z

Turner, B. L., Papházy, M. J., Haygarth, P. M., and Mckelvie, I. D. (2002). Inositol Phosphates in the Environment. Philos. *Trans. R. Soc B. Biol. Sci.* 357, 449–469. doi: 10.1098/rstb.2001.0837

Van Mooy, B. A. S., Krupke, A., and Dyhrman, S. T. (2015). Major Role of Planktonic Phosphate Reduction in the Marine Phosphorus Redox Cycle. *Science* 348, 783–785. doi: 10.1126/science.aaa8181

Vershinina, O. A., and Znamenskaya, L. V. (2002). The Pho Regulons of Bacteria. *Microbiology* 71, 497–511. doi: 10.1023/A:1020547616096

Wanner, B. L. (1993). Gene Regulation by Phosphate in Enteric Bacteria. *J. Cell. Biochem.* 51, 47–54. doi: 10.1002/jcb.240510110

Watson, S. J., Cade-Menun, B. J., Needoba, J. A., and Peterson, T. D. (2018). Phosphorus Forms in Sediments of a River-Dominated Estruary. *Front. Mar. Sci.* 5. doi: 10.3389/fmars.2018.00302

White, R. H., and Miller, S. L. (1976). Inositol Isomers: Occurrence in Marine Sediments. *Science* 193, 885–886. doi: 10.1126/science.193.4256.885

Zhang, Y. S., Werner, W., Scherer, H. W., and Sun, X. (1994). Effect of Organic Manure on Organic Phosphorus Fractions in Two Paddy Soils. *Biol. Fertil. Soils* 17, 64–68. doi: 10.1007/BF00418674

Ziebis, W., McManus, J., Ferdelman, T., Schmidt-Schierhorn, F., Bach, W., Muratli, J., et al. (2012). Interstitial Fluid Chemistry of Sediments Underlying the North Atlantic Gyre and the Influence of Subsurface Fluid Flow. *Earth Planet. Sci. Lett.* 323-324, 79–91. doi: 10.1016/j.epsl.2012.01.018

Conflict of Interest: The authors declare that the research was conducted in the absence of any commercial or financial relationships that could be construed as a potential conflict of interest.

Publisher's Note: All claims expressed in this article are solely those of the authors and do not necessarily represent those of their affiliated organizations, or those of the publisher, the editors and the reviewers. Any product that may be evaluated in this article, or claim that may be made by its manufacturer, is not guaranteed or endorsed by the publisher.